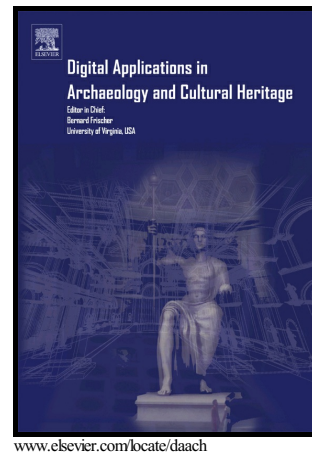


Author's Accepted Manuscript

Assessing earthquake effects on archaeological sites: the employment of photogrammetry and 3D model analysis

Paolo Forlin, Riccardo Valente, Miklós Kázmér



PII: S2212-0548(17)30063-2
DOI: <https://doi.org/10.1016/j.daach.2018.e00073>
Reference: DAACH73

To appear in: *Digital Applications in Archaeology and Cultural Heritage*

Received date: 2 December 2017
Revised date: 16 February 2018
Accepted date: 26 April 2018

Cite this article as: Paolo Forlin, Riccardo Valente and Miklós Kázmér, Assessing earthquake effects on archaeological sites: the employment of photogrammetry and 3D model analysis, *Digital Applications in Archaeology and Cultural Heritage*, <https://doi.org/10.1016/j.daach.2018.e00073>

This is a PDF file of an unedited manuscript that has been accepted for publication. As a service to our customers we are providing this early version of the manuscript. The manuscript will undergo copyediting, typesetting, and review of the resulting galley proof before it is published in its final citable form. Please note that during the production process errors may be discovered which could affect the content, and all legal disclaimers that apply to the journal pertain.

Assessing earthquake effects on archaeological sites: the employment of photogrammetry and 3D model analysis

Paolo Forlin, Riccardo Valente, Miklós Kázmér

1. Introduction

Earthquake archaeology (or archaeoseismology) is a relatively young and emerging discipline which aims to study past seismic disasters through evidence from the archaeological record (Stiros and Jones 1996; Galadini et al. 2006; Ambraseys 2006). The main goal of archaeoseismology is to identify evidence with the potential to shed new light on the occurrence and characteristics of ancient earthquakes while providing data to inform seismic risk assessment programmes (Sintubin and Stewart 2008, Caputo and Helly 2008).

Fundamentally, the discipline attempts to detect seismic effects in archaeological contexts. At the core of the research agenda, therefore, are the creation of typological catalogues of earthquake damage to archaeological sites and ancient standing structures (Kazmer 2015, Marco 2008). Such features, including penetrative fractures within standing walls, structural deformation, *in situ* destruction layers, evidence of fire, to name only a few, were recently labelled as Earthquake Archaeological Effects (EAEs: Rodríguez-Pascua et al. 2011). The identification of EAEs is challenging and not always unequivocal. As widely reported by the cited literature, when analysing seismic damage on archaeological sites, it is fundamental to: (i) recognise the seismic origin of a feature and (ii) rule out any other possible cause for such evidence (Marco 2008:149). This means that the documentation of damage must be as accurate and detailed as possible. So far, archaeoseismological fieldwork has tended to document earthquake evidence through descriptive summaries of the identified features illustrated with a number of generic pictures. Evidently, an archaeological approach to seismic damage, e.g. making use of plans, orthophotos and profiles, is commonly not applied. On the other hand, field archaeology tends not to document in detail (or even fail to identify) seismic damage, not providing or lacking fundamental information for the comprehension of a site's evolution.

Our paper proposes an operational framework based on the application of digital photogrammetry and 3D analysis of seismically affected archaeological sites in order to enhance the typical methodology.

The intensive development of image-based modelling in recent years has created a wide variety of applications which hold the potential to accelerate and improve traditional research methods. The contribution of Computer Vision algorithms such as Structure from Motion (SfM) have revolutionised traditional photogrammetry, allowing a quicker and more user-friendly workflow to produce 3D reconstructions, orthophotos and Digital Elevation Models (DEMs). Archaeology is one scientific discipline which particularly benefits from the application of digital photogrammetry for the purposes of documentation, reconstruction and dissemination.

Digital photogrammetry has been successfully applied to the documentation of archaeological layers for more than a decade (Pollefeys et al., 2000; Pollefeys et al., 2001; and Cosmas et al., 2001). The development and proliferation, in recent years, of commercial software allowing largely automatic image processing has facilitated the successful application of digital photogrammetry to even large-scale excavation areas (De Reu et al., 2013; Dellepiane et al., 2013; Olson et al., 2013; De Reu et al., 2014; Stal et al., 2014).

The application of digital photogrammetry to the documentation of historic standing buildings follows a long-standing tradition of the use of terrestrial close-range photogrammetry in architectural recording. Its high flexibility expanded the possibilities of recording and analysis of buildings, integrating 2D (orthophotos), 2.5D (DEMs) and 3D (meshes) outputs. Orthophotos can be very effective in the recording of standing structures, since they provide a reliable photographic record of faces and a basis for traditional elevation drawings (Yastikli, 2007; Barsanti et al., 2013). When generated from images acquired using UAV platforms, they can also incorporate close-range-aerial imagery (Colomina and Molina, 2014; Balletti et al., 2015). Moreover, section lines extracted from 3D meshes can be set in order to obtain profiles of the reconstructed structures (Green et al., 2014:177).

Three-dimensional survey technologies, such as terrestrial laser scanner (TLS) and digital photogrammetry, are currently widely used in the recording of built heritage. Both techniques are highly reliable in both measurement accuracy and morphological analysis (Bayram et al., 2015; Galeazzi, 2016; Sapirstein, 2016; Teza, Pesci and Ninfo, 2016). TLS, along with other technologies, is often applied to the structural monitoring of archaeological sites (Peloso, 2005:214-218; Tapete et al., 2013). Digital photogrammetry, combined with other surveying techniques, has been widely applied to structural assessment (Arias et al., 2005; Arias et al., 2007; Sánchez-Aparicio et al., 2015) and the recording of cracks in ancient masonry (Armesto et al., 2008; Alshawabkeh & El-Khalili, 2013).

The extraction of masonry profiles from photogrammetric sources has been investigated by Fujii et al. (2009) to assess structural damage to archaeological buildings, assessing in this case the damage caused to the structures by weather erosion.

Not surprisingly, both TLS and digital photogrammetry, along with other quantitative methods, have also been applied to earthquake effects analysis (Hinzen et al., 2011: 32-34; Hinzen et al., 2013; Schreiber et al., 2009 for instance) or, more broadly, to seismically damaged structures (see for instance Arrighetti 2015:142-152 for photogrammetry; Bertocci et al., 2015 for the application of TLS). In fact, the use of photogrammetry to document cultural heritage affected by seismic damage has a long-standing tradition. In Italy, for example, several photogrammetric campaigns were carried out for the purpose of documentation after the severe earthquakes which affected the Friuli Venezia Giulia region in 1976 (De Luca, 1987-1988; Foramitti, 1977).

The overall aim of this study is to evaluate, for the purposes of archaeoseismology, to what extent such methodologies can provide or facilitate (i) rapid but accurate records

of analysed archaeological contexts, (ii) three-dimensional reconstructions, (iii) the documentation of archaeological features by means of plans, sections, and elevations, and (iv) the extraction of additional information and data for archaeoseismological analysis.

This paper draws on evidence from two case studies of the EU-funded ArMedEa project (Archaeology of Medieval Earthquakes in Europe, 1000-1550 AD; Forlin, Gerrard, Petley 2015).

2. Material and method

2.1 Case studies: Saranda Kolones (Cyprus) and El Castillejo (Spain)

This study focuses on two case studies: (i) the crusader castle of Saranda Kolones (Paphos, Cyprus) and (ii) the Islamic fortified village of 'El Castillejo' (Guajar Faragüit, Granada, Spain) (**fig. 1**)

El Castillejo – Guajar Faragüit (Granada, Spain)

El Castillejo is a fortified village dating to the Islamic period built on the top of an isolated hill facing the village of Guajar Faragüit (Granada, Spain). The extent of the site (about 1.5 ha, 120 x 130 m) is delineated by a circuit wall with an integrated *baluarte* (fortified gate) on the western side (**fig. 2A**).

Today, at least twelve buildings across the site are in a partially standing condition. Excavations undertaken by the University of Granada from the 1980s until 2001 demonstrate that the site was occupied from the beginning of the 11th century to the mid-14th century (García Porras, A, 2001; Bertrand et al., 1990; Malpica et al., 1985; Malpica et al., 1986; Malpica and Cressier 1989). The buildings conform to a repeated plan of several rooms organized around a central patio with at least two floors. Standing walls were built in rammed earth, known locally as *tapial*, with foundations of stone masonry. The reason behind the abandonment of the village remains controversial (one possibility is that its desertion was caused by the Black Death; Malpica and Cressier 1989), but, at some point during its occupation, possibly during the 13th - early 14th century, El Castillejo experienced a destructive earthquake. Seismic damage occurred across the site with a focus in the eastern area, which was almost completely destroyed and, unlike the rest of the site, never subsequently resettled. The western area survived the seismic event with minor damage, with clear EAEs recognisable in the surviving standing structures. Furthermore, in this area, a number of buildings and the circuit wall display evidence of the post event repairs through a later phase of *tapial*, of lower quality than the earlier phases, and the reemployment of *spolia* and material from the earlier period. The present study focuses on Building 4, a 5-storey dwelling measuring about 10m x 11m (**fig. 2B**).

The central core of this structure consists of four massive walls delimiting an area of 7 x 7 m. Three annexes were added to this central structure: a small room built along the eastern side, close to the entrance, and two other annexes flanking the southern side. These structures display a differential state of preservation. The walls of the

outer annexes are poorly preserved, as well as the walls delimiting the inner rooms of the building. By contrast, three out of the four structures delimiting the central part of the dwelling are still standing and reach a maximum height of 3.6m. The northern wall, by contrast, collapsed almost completely, and only the foundations terracing the surface downslope remain *in situ*. As a consequence of the state of preservation, earthquake archaeological effects are recognisable on walls 401 (western side), 405 (eastern side), and 408 (southern side).

Seismic damage consists of a variety of penetrative fractures such as horizontal, vertical and shear cracks with some evidence of the shifting of rammed earth blocks (**fig. 3**).

Wall 408, the southern wall of Building 4, contains a huge penetrative, shear crack crossing the entire height of the structure. It can be observed as an individual feature on the external wall (408-south), but it is associated with minor (shear and vertical) cracks on the internal wall face (408-north). The western wall of the building (405) shows other, huge shear cracks associated –as in the case with 408- with vertical, sub-vertical and sub-horizontal fractures. Wall 401, the structure's western wall, preserves evidence of seismic damage represented by a composite network of vertical, sub-vertical and horizontal fractures. The upper *tapial* block is displaced and rotated, a point which can be clearly observed from the external profile of the wall. As already mentioned, at some point the building's northern wall (404) entirely collapsed, and no EAEs are recognisable on the *in situ* foundations.

Saranda Kolones (Paphos, Cyprus)

Saranda Kolones is a fortified crusader castle built at the beginning of the 13th century to protect the harbour of Paphos (Cyprus) (Petre 2012). Soon after its construction on solid rock, in AD 1222, a violent earthquake razed the fortification to the ground. The seismic destruction of the castle was recorded in contemporary historical accounts (reported in Ambraseys 2009; Guidoboni and Comastri 2005) and is confirmed by archaeological evidence. Excavations carried out between 1957 and 1980s (Megaw 1957, 1972, 1994; Rosser 1985, 1986) recovered extensive layers of destruction (comprising debris, fallen masonry and displaced blocks) and the presence of both human and animal victims beneath the rubble (Rosser 2004).

The archaeological remains of the castle (**fig. 4**) are characterised by a concentric plan with (i) a pentagonal outer ward (about 75 m across) with rounded or polygonal corner towers and rectangular or wedge shaped interval towers, (ii) an inner rectangular ward (35m x 37m) with projecting, rectangular towers at each corner and a D-shaped tower in the centre of the eastern wall, (iii) an internal courtyard delimited by nine rectangular, massive pillars, three of them hosting a pair of latrines (Petre 2012). Pillars' bases are still preserved *in situ* up to a height of about 3 meters. Clear EAEs such as penetrative cracks, lateral displacements, tilting and wall detachments are still recognisable on a number of the castle's structures.

Our study takes into consideration the remains of two internal pillars, namely pillars 1 and 2, corresponding with the structures located at the NW corner of the castle's inner court (see **fig. 4** for their locations).

Pillar 1 (**Fig. 5**) is a massive quadrangular structure (measuring 3.68m x 3.67m) hosting two opposing latrines on the north and south sides. Pillar 2 (**Fig. 5**) is a rectangular pillar measuring 3.47m x 2.15m connected to the castle's kitchen along its northern face. Both structures are only partially preserved, their upper parts having collapsed as a result of the AD 1222 earthquake. The remains of pillar 1 reach a maximum height of 3.29m, while pillar 2 is only preserved up to 2.35m. One corner of pillar 1 appears to have been heavily restored by means of cobble stones.

Despite the state of preservation of the pillars, EAEs are clearly visible throughout the structures. Pillar 1 is widely affected by sub-vertical cracks running across several courses of ashlar and masonry blocks. The latrines were also seismically-affected, with both the internal walls and toilet seats fractured by vertical cracks. The structure, as a whole, is deformed by vertical compression and, as a result of the vertical seismic loads, the structure's faces are extruded in profile. Pillar 2 is poorly preserved, with only five courses of the structure remaining *in situ*. The pillar's western and eastern faces show a collapse interface corresponding with a distinctive shear feature, with the surviving elements containing a shear fracture cross-cutting multiple courses of ashlar. This penetrative fracture is associated with a right-lateral displacement.

2.2 3D reconstruction

In order to assess the seismic damage preserved on the selected structures at El Castillejo and Saranda Kolones, both digital photogrammetry and 3D modelling software were employed. Digital photogrammetry has been devoted to in-field surveying, while 3D approaches were applied in the subsequent analysis phase. The photogrammetry phase was performed using Agisoft PhotoScan, while the 3D modelling phase was carried out using Rhinoceros 5. Digitalisation of the identified seismic features was then obtained with Adobe Illustrator CC.

Photogrammetric Survey

In order to record building 4 at El Castillejo, 535 photographs were taken. A high number of images was necessary to ensure the required overlap between different images, allowing high levels of detail in both meshes and textures. Once processed using PhotoScan, the resulting 3D mesh surface was composed of 1,291,748 faces and 658,183 vertices. For the El Castillejo site, an overall number of 24 Ground Control Points (GCPs), using coded targets generated by PhotoScan, were set all around building 4; this allowed accelerated surveying operations and improved accuracy of the final georeferencing. GCPs were measured using a total station (TS), with local coordinates. The overall error estimated by the software is 0.015 metres. On-site activities (photographic documentation and GCPs measurement) required about 3 hours.

In the case of Saranda Kolones, separate photogrammetric projects were created for each pillar. For example, the model of pillar 1 was created from 238 images, resulting in a final mesh of 1,028,998 faces and 515,773 vertices; for pillar 2, 94 images were processed, producing a final mesh of 338,329 polygons and 182,895 vertices. The disparity in the number of input images between the pillars relates to the greater

geometric complexity and size of pillar 1. In this case, GCP coordinates were extracted from a TS survey of the entire archaeological site carried out in 2002-2003 by 'The Saranta Kolones Excavations Project' (surveyor: Richard Anderson; directors: John Hayes and Archibald Dunn, Centre for Byzantine, Ottoman and Modern Greek Studies, University of Birmingham). The photographic documentation of the two pillars required less than one hour.

Images of structures from both sites were taken with a non-calibrated Nikon D5300 SLR camera, equipped with a Nikkor 18-140 mm f/3.5-5.6G ED AF-S VR DX lens.

Three-dimensional data extraction and analysis

The three-dimensional surfaces produced through the photogrammetry process resulted in detailed and highly accurate models with which to perform advanced analysis.

Digital Elevation Models (DEMs) were employed in order to enhance the damage patterns and deformations caused by seismic loads. The surfaces of wall 408 from El Castillejo and pillar 2 from Saranda Kolones were selected. The extraction of the DEMs required the original coordinates from the instrumental survey to be processed in order to turn the selected vertical surfaces into horizontal ones. Raster files were automatically generated by PhotoScan after the upload of the new coordinates.

As one of the main goals of the project was to record and recognize evidence of seismic damage directly on the structures, with particular focus on areas which were difficult to reach and observe in the field, a series of vertical and horizontal sections were extracted from the three-dimensional models.

In order to do this, the meshes were imported into the modelling software Rhinoceros 5. The meshes maintain their georeferencing parameters, meaning that no additional operations, such as roto-traslation or scaling, are required. In order to assess whether ancient seismic damage was detectable in the digital model, a series of section lines were set, in order to intercept those parts of the structures with a high density of visible cracks. These section lines were perpendicular to the mesh and parallel to each other. Once the direction of the section line is set, the software automatically extracts the relative section which runs over the entire surface, virtually slicing the built structures: this method allows the extraction of highly detailed sections (similar to those created through the processing of laser scan data) which are difficult to achieve through traditional survey techniques.

The graphical outputs, i.e. sections, were laid out directly in Rhinoceros software and completed with measurements.

3. Results

3D reconstructions of the selected case studies were employed in order to enhance the archaeoseismological analysis by means of mesh and DEMs analysis, orthophoto

characterisation, plan and section extraction. Results are discussed below by case study.

3.1 El Castillejo

The 3D model produced through the methodology discussed above (**Fig. 6**) clearly reproduces the seismic damage observed in the field.

Firstly, orthophotos extracted from the generated 3D model permit the shape and spatial organisation of the seismic cracks to be visualised. In particular, **fig. 7** illustrates the pattern of cracks visible on wall 408, allowing the penetrating nature of the damage as shown by the comparison between the inner, northern side and its reversed counter face to be appreciated.

Secondly, in addition to the immediately noticeable complex pattern of seismic cracks within the photogrammetric output, the 3D model allows a detailed assessment of other, less obvious EAEs. These are revealed through the extraction of a series of section/profiles from the photogrammetric 3D mesh. These cracks, intersecting large adobe blocks and running horizontally at about 30 degrees from the horizontal (arrows), are evidence for the lateral shaking of the buildings, as a result of forces acting approximately perpendicular to the walls.

Given the height of the surviving masonry and the mechanical characteristics of the construction techniques (rammed earth), several intersecting sections were set in order to assess the different types of damage. Two parallel vertical sections oriented from east to west (A-A' and B-B': **fig. 8**) were extracted from the mesh, as well as an additional pair of parallel sections oriented from north to south (C-C' and D-D'; **fig. 9**), intercepting the majority of the standing wall of the structure. A final horizontal section was set 2.1m from the ground.

The vertical sections accurately reproduce the walls' profiles, exhibiting detailed seismic damage. For example, section AA' shows the profiles of cracks and a post hole on the upper part of wall 401 with another crack at the base of wall 407. Section BB', along with another two post holes, permits the clear identification of the outward displacement of the upper rammed earth block of wall 401 and a pattern of shear crack profiles in wall 405. [Section AA', wall 401: west side, 1.5 cm; east side, 4.5 cm. Section BB', wall 401: west side, 4.5 cm (displacement). Section BB', wall 405: west side, 9 cm; east side: 4.5 and 3.5 cm.]

The north-south oriented sections CC' and DD' highlight the pattern of penetrative cracks in wall 408 as well as some very shallow damage in residual walls 402 and 403. [Section CC', wall 408: south side, 1.5 cm; north side, 0.5 cm. Section DD', wall 408: south side, 7 cm; north side, 7.5 cm.]

Penetrative cracks are also visible in the profiles extracted from the horizontal sections (**fig. 10**) This is the case with walls 401 and 408, in which the many irregularities visible along the walls' profiles correspond with the observed seismic cracks [Horizontal section, wall 408: north side, 7.5 cm]. Such profiles permit accurate measurements of the cracks within the standing structures to be taken.

Compared with measurements taken in the field, the dimensions of these cracks extracted from the 3D mesh are highly reliable.

The understanding of the seismic damage pattern and its visualisation can also benefit from the extracted Digital Elevation Model (DEM). **Fig. 11** and **12** show the DEM of the southern face of wall 408 visualised in hillshade and slope mode.

From an archaeoseismological perspective, it has to be noted that penetrative cracks crossing more than one block associated with out-of-plane shifting suggest (according to the scale proposed by Rodríguez-Pascua et al., 2013) a minimum intensity value IX EMS98 (destructive). The damage observed by the excavators in the eastern part of the site, which went almost completely destroyed, confirm the assessment provide by the analysis of the still standing structures.

3.2 Saranda Kolones

The 3D reconstructions of pillar 1 and 2 from the Crusader castle at Saranda Kolones exhibit an impressive correspondence with the stone-by-stone instrumental survey gently provided by ‘The Saranta Kolones Excavations Project’. Vector contours plotted during that survey were then superimposed on the 3D photogrammetric reconstructions of the two pillars, confirming the accuracy of both outputs (**Fig. 13**). The overall error estimated by the software is 0.013 m for pillar 1 and 0.007 m for pillar 2.

As in the case of El Castillejo, orthophotos offer an extremely useful method to map seismic damage across the different parts of the structures. This is shown in **figure 14** which displays the visible EAEs on the northern sides of pillar 1 and on the western side of pillar 2.

The 3D meshes produced through photogrammetry of pillar 1 and 2 also facilitate an in-depth archaeoseismological analysis. Again, seismic damage such as shear and sub-horizontal cracks are clearly discernible within the 3D model. **Figure 15**, for instance, compares a close-up picture of a shear crack associated with lateral shifting in pillar 2 with the resulting 3D model. A series of parallel horizontal sections drawn, at different heights, through pillar 1 and 2 allow observation of the degree of cracking and displacement which have affected the structure. Sections A and B from pillar 2 (**fig. 16**) show centimetre-scale displacement of masonry blocks on both sides of the structure at 0.25 m (A) and 1.10 m (B) above floor level. The displacement extracted from the 3D model (1.5 to 3.3 cm) corresponds with the misalignment measured in the field. The extracted DEM visualises the same displacement, enhancing the out-of-plane shifting of the upper part of the pillar’s surviving structure. **Fig. 17** shows the intrusion of the upper blocks on the eastern side and, on the other hand, the extrusion of the upper portion on its western side. This deformation augments upward and is clearly associated with the shear, penetrative fracture detectable on the structure.

This evidence is highly significant, as deformation cutting across a pillar and the uniformity of deformation in adjacent pillars (the same effect was identified on Pillar 1) are a certain indication of earthquake action. A displacement as minor as 1-4 cm

along fractures over more than 2 m width of the pillar seems hardly noteworthy. However, the uniform, right-lateral nature of the displacement - however small - in four, parallel pillar faces has a significant meaning: deformation was not random but systematic. The only force capable of acting on all four faces simultaneously is seismic shaking. Further archeoseismic features consist of a number of cracked masonry (single and multiple blocks, Figs 5, 13,15). Intensity grade VII is assigned to these deformations (Rodríguez-Pascua et al., 2013), whereas masonry blocks shifted perpendicularly to the wall (out-of-plane deformation; Figs 5, 13, 15) indicate an earthquake of minimum intensity IX EMS98 (very destructive). The massive destruction layers sealing the surviving structures of the castle corroborate this assessment. Eventually, 3D modelling makes it less likely that such small but significant features may be overlooked.

4. Discussion

In both case studies, photogrammetric reconstructions of the selected structures (i) support archaeoseismological analysis and (ii) provide additional information for the assessment of earthquake damage. As the initial meshes have been accurately georeferenced, the various outputs produced, i.e. prospects, orthophotos as well as horizontal and vertical sections, are both accurately scaled and fully measurable, while the different angles of the structural elements are clearly displayed and can be estimated through digital measurements.

Orthophotos of elevations allow the accurate mapping of earthquake archaeological effects. This is particularly the case when comparing opposing faces affected by penetrative cracks. In short, orthophotos offer a reliable tool to assess the impact of seismic effects and to record and visually reproduce these features.

Photogrammetric 3D meshes and DEMs permit the analysis to be advanced a further step forward. Profiles extracted from 3D models, for example, allow the accurate measurement of damage caused by seismic load, notably (i) the lateral displacement of masonry portions or *tapial* blocks and (ii) the depth and spatial organisation of the penetrative fractures. As shown, measurements extracted from the 3D reconstructions are consistent with those taken in the field. This means that archaeoseismological analysis can benefit from the analysis of 3D models through the accurate measurement of seismic damage, in particular those features which are difficult or impossible to access in the field (for example due to their height). Another positive aspect is the ability to set section lines through the most significant parts of a digital model as required. The lines can be set virtually at any point in the structure, regardless of real-world obstacles. Additionally, cracks and displacements are easily recognizable on masonry surfaces although the depth of penetration is often difficult to measure on structures much larger than a person. This kind of surveying is relatively cost-effective if compared to laser scanning, and can normally be carried out by a single operator in a reasonably short timeframe. As aforementioned, the on-site activity took an overall period of about three hours at El Castillejo and one hour at Saranda Kolones. Ultimately, cracks organisation can also displayed three-

dimensionally, showing the penetrative nature of the seismic fractures, as shown for wall 408 of Building 4 in El Castillejo (**fig. 18**).

The level of detail obtained from the reconstructed three-dimensional models is remarkable and the measurements of the calculated damage appear highly reliable (see **Table 1**). Through our analysis, we can demonstrate the effectiveness of highly detailed photogrammetric reconstructions for the purposes presented in this paper. Regarding the seismic cracks and lateral displacements observed in our case studies, 3D photogrammetry and modelling reduce the chance that such small but significant features might be overlooked. While relevant out-of-plane damage can also be easily recorded through traditional methods, small-scale and scattered damage are difficult to reproduce and are usually plotted on two-dimensional images. Moreover, even if cracks and other damage can be measured and assessed in the field, they can still be difficult to reproduce in traditional sections.

Importantly, not all the EAEs detected on the structures discussed above have been reproduced by the digital models, namely superficial and small cracks which are also important to assess, although the textures produced have helped in their identification. Meshes should always be carefully checked since surface gaps due to missing data (such as portions of structures which are too high to be photographed) are often automatically filled by the software, reconstructing these parts in an inaccurate way. In addition, photogrammetric surveys should always be accompanied by a topographic survey as this allows accuracy to be confirmed and correct georeferencing.

5. Conclusions

The methodology discussed above demonstrates the high potential of 3D models in the display, detection and interpretation of structural irregularities.

Furthermore, the results obtained from the analysis of three-dimensional structural models are promising and clearly illustrate the validity of these methods. The meshes produced were sufficiently detailed to record and highlight damage up to the order of a few centimetres. Wall morphology and damage can be reproduced not only using photographic textures, but also by DEMs and the mesh itself, allowing the extraction of vertical and horizontal profiles from structures where the effects of seismic damage can be clearly recognized.

The resulting 3D images combined with traditional photographs allow the user to 'bring the site home'. Using these methods, many details can be observed and measured simply by looking at the computer screen, extending and enhancing a researcher's ability to examine the site beyond the, often limited, time available in the field.

Captions:

Fig. 1. Map showing the location of the archaeological sites discussed in the text.

Fig. 2. El Castillejo, Guájar Faragüit (Granada, Spain). Aerial photo (© Google Earth) and general view of Building 4 from north-east.

Fig. 3. El Castillejo. Seismic damage visible on the standing structures of Building 4.

Fig. 4. Saranda Kolones (Paphos, Cyprus). Aerial view showing the location of pillars 1 and 2 within the fortification (photo: ArMedEa project).

Fig. 5. Saranda Kolones. Pillar 1 and Pillar 2 showing distinctive seismic damage.

Fig. 6. El Castillejo, Building 4. Mesh and texturised mesh of the standing walls.

Fig. 7. El Castillejo, Building 4, Wall 408. Orthophotos and vectorialised elevation of the seismic damage visible on the northern and southern (reversed) faces.

Fig. 8. El Castillejo, Building 4. East-west oriented sections of the obtained mesh. Seismic damage is shown and emphasised by red circles. Block displacement and the depth of the penetrative fractures from the corresponding face are expressed in millimetres.

Fig. 9. El Castillejo, Building 4. North-south oriented sections of the obtained mesh. Seismic damage is shown and emphasised by red circles. The depth of the penetrative fractures from the corresponding face are expressed in millimetres.

Fig. 10. El Castillejo, Building 4. Horizontal section of the obtained mesh. Seismic damage is shown and emphasised by red circles. The depth of the penetrative fractures from the corresponding face are expressed in millimetres.

Fig. 11. El Castillejo, Building 4, Wall 408 (south side). The extracted DEM (A) allows to appreciate the penetrative fractures when visualised in hillshade (B) and slope (C) mode.

Fig. 12. El Castillejo, Building 4, Wall 408 (south side). Close-up of shear penetrative cracks visualised in hillshade (A) and slope (B) mode.

Fig. 13. Saranda Kolones. Superimposition of the vector contours plotted by the 'Saranda Kolones Excavations Project' on the 3D photogrammetric reconstructions of the two pillars.

Fig. 14. Saranda Kolones. Orthophotos and vectorialised elevation of the seismic damage visible on Pillar 1 (north face) and Pillar 2 (west face).

Fig. 15. Saranda Kolones, pillar 2, western side. Comparison between a close-up of a shear crack associated with lateral shifting (A) with the resulting 3D model (B).

Fig. 16. Saranda Kolones, pillar 2. Sections A2 and B2 showing centimetre-scale displacement of masonry blocks on both sides of the structure. The picture on the right records the out-of-plane shifting along the eastern side of the pillar.

Fig. 17. Saranda Kolones, pillar 2. DEM of the east and west sides emphasising the seismic deformation of the structure. DEM is visualised by means of a slope visualisation overlaid by a colour ramp in transparency.

References

Al-kheder, S., Al-shawabkeh, Y., & Haala, N., 2009. Developing a documentation system for desert palaces in Jordan using 3D laser scanning and digital photogrammetry. *Journal of Archaeological Science*, 36(2), 537–546. <http://doi.org/10.1016/j.jas.2008.10.009>

Alshwabkeh, Y., & El-Khalili, M., 2013. Detection and quantification of material displacements at historical structures using photogrammetry and laser scanning techniques. *Mediterranean Archaeology and Archaeometry*, 13(2), 57–67.

Ambraseys, N. N., 2009. Earthquakes in the Mediterranean and Middle East: a multidisciplinary study of seismicity up to 1900. Cambridge

Armesto, J., Arias, P., Roca, J., & Lorenzo, H., 2008. Monitoring and Assessing Structural Damage in Historic Buildings. *The Photogrammetric Record*, 23(121), 36–50.
<http://doi.org/10.1111/j.1477-9730.2008.00466.x>

Arias, P., Herráez, J., Lorenzo, H., & Ordóñez, C., 2005. Control of structural problems in cultural heritage monuments using close-range photogrammetry and computer methods. *Computers & Structures*, 83(21-22), 1754–1766.
<http://doi.org/10.1016/j.compstruc.2005.02.018>

Arias, P., Armesto, J., Di-Capua, D., González-Drigo, R., Lorenzo, H., & Pérez-Gracia, V., 2007. Digital photogrammetry, GPR and computational analysis of structural damages in a mediaeval bridge. *Engineering Failure Analysis*, 14(8), 1444–1457.
<http://doi.org/10.1016/j.engfailanal.2007.02.001>

Arrighetti, A., & Cavalieri, M., 2012. Il rilievo fotogrammetrico per nuvole di punti RGB della sala triabsidata del sito archeologico di Aiano-Torraccia di Chiusi (SI). *Archeologia e calcolatori*, (23), 121-134.

Arrighetti, A., 2012. Tecnologie fotogrammetriche e registrazione 3D della struttura materiale: dal rilievo alla gestione dei dati. *Archeologia e Calcolatori*, 23, 283-296.

Arrighetti, A., 2015. L'archeosismologia in architettura. Per un manuale. Firenze University Press, Firenze

Balletti, C., Guerra, F., Scocca, V., & Gottardi, C., 2015. 3D INTEGRATED METHODOLOGIES FOR THE DOCUMENTATION AND THE VIRTUAL RECONSTRUCTION OF AN ARCHAEOLOGICAL SITE. In *Int. Arch. Photogramm. Remote Sens. Spatial Inf. Sci.*, (Vol. XL-5/W4, pp. 215–222).
<http://doi.org/10.5194/isprsarchives-XL-5-W4-215-201>

Barazzetti, L., Binda, L., Scaioni, M., & Taranto, P., 2011. Photogrammetric survey of complex geometries with low-cost software: Application to the 'G1' temple in Myson, Vietnam. *Journal of Cultural Heritage*, 12(3), 253–262.
<http://doi.org/10.1016/j.culher.2010.12.004>

Barazzetti, L., & Scaioni, M., 2014. Reality-Based 3D Modelling from Images and Laser Scans: Combining Accuracy and Automation. (F. V. Cipolla-Ficarra, Ed.) *Advanced Research and Trends in New Technologies, Software, Human-Computer Interaction, and Communicability*. IGI Global. <http://doi.org/10.4018/978-1-4666-4490-8>

Barsanti, S. G., Remondino, F., & Visintini, D., 2013. 3D Surveying and Modeling Of Archaeological Sites. In *ISPRS Annals of the Photogrammetry, Remote Sensing and Spatial Information Sciences* (pp. 145–150). XXIV International CIPA Symposium.

Bayram, B., Nemli, G., Özkan, T., Oflaz, O. E., Kankotan, B., & Çetin, İ., 2015. Comparison Of Laser Scanning And Photogrammetry And Their Use For Digital Recording Of Cultural Monument Case Study: Byzantine Land Walls-Istanbul. *ISPRS Annals of Photogrammetry, Remote Sensing and Spatial Information Sciences*, II-5/W3, 17–24. <http://doi.org/10.5194/isprsannals-II-5-W3-17-2015>

Bertocci, S., Minutoli, G., Pancani, G., 2015, Rilievo tridimensionale e analisi dei dissesti della Pieve di Romena, *Disegnarecon*, 8, 26.1-26.20

Bertrand, M, Cressier, P, Malpica, A, Rosselló, G, 1990. La vivienda rural medieval de “El Castillejo” (Los Guájares, Granada), in *La casa hispano-musulmana. Aportaciones de la arqueología*, Granada, 207-227

Bitelli, G., & Girardi, F., 2010. Problematiche nel rilievo e modellazione tridimensionale di oggetti di piccole dimensioni nel campo dei Beni Culturali, in *Atti 14a Conferenza ASITA*, Brescia, Italy, 9-12.

Colomina, I., & Molina, P., 2014. Unmanned aerial systems for photogrammetry and remote sensing: A review. *ISPRS Journal of Photogrammetry and Remote Sensing*, 92, 79–97. <http://doi.org/10.1016/j.isprsjprs.2014.02.013>

Cosmas, J., Itegaki, T., Green, D., Grabczewski, E., Weimer, F., Van Gool, L., Zalesny, A., Vanrintel, D., Leberl, F., Grabner, M., Schlinder, K., Karner, K., Gervautz, M., Hynst, S., Waelkens, M., Pollefeys, M., DeGeest, R., Sablatnig, R. & Kämpel, M., 2001. 3D MURALE: a multimedia system for archaeology. In *Proceedings of the 2001 conference on Virtual reality, archeology, and cultural heritage*, 297-306. <http://dx.doi.org/10.1145/584993.585048>.

Dellepiane, M., Dell’Unto, N., Callieri, M., Lindgren, S., & Scopigno, R., 2013. Archeological excavation monitoring using dense stereo matching techniques. *Journal of Cultural Heritage*, 14(3), 201–210. <http://dx.doi.org/10.1016/j.culher.2012.01.011>.

De Luca, S., 1987-1988. Fotogrammetria e recupero nei centri storici terremotati del Friuli: Gemona, Venzone, Artegna, *Bollettino dell’Associazione “Amici di Venzone”*, a. XVI-XVII.

De Reu, J., Plets, G., Verhoeven, G., De Smedt, P., Bats, M., Cherretté, B., De Maeyer, W., Deconynck, J., Herremans, D., Laloo, P., Van Meirvenne, M. & De Clerq, W., 2013. Towards a three-dimensional cost-effective registration of the archaeological heritage. *Journal of Archaeological Science*, 40(2), 1108-1121. <http://dx.doi.org/10.1016/j.jas.2012.08.040>.

De Reu, J., De Smedt, P., Herremans, D., Van Meirvenne, M., Laloo, P., & De Clercq, W., 2014. On introducing an image-based 3D reconstruction method in archaeological excavation practice. *Journal of Archaeological Science*, 41, 251-262. <http://dx.doi.org/10.1016/j.jas.2013.08.020>.

Doneus, M., Verhoeven, G., Fera, M., Briese, C., Kucera, M., & Neubauer, W., 2011. From deposit to point cloud—a study of low-cost computer vision approaches for the straightforward documentation of archaeological excavations. *Geoinformatics FCE CTU*, 6, 81-88. <http://dx.doi.org/10.14311/gi.6.11>.

Kaufman, J., Rennie, A. E., & Clement, M., 2015. Single Camera Photogrammetry for Reverse Engineering and Fabrication of Ancient and Modern Artifacts. *Procedia CIRP*, 36, 223-229.

Kersten, T. P., & Lindstaedt, M., 2012. Image-based low-cost systems for automatic 3D recording and modelling of archaeological finds and objects. In *Progress in cultural heritage preservation* (pp. 1-10). Springer Berlin Heidelberg.

Fiorini, A., Urcia, A., & Archetti, V., 2011. The digital 3D survey as standard documentation of the archaeological stratigraphy. In *VAST 2011: The 12th International Symposium on Virtual Reality, Archaeology and Cultural Heritage*, 145-152. Eurographics Association. <http://dx.doi.org/10.2312/VAST/VAST11/145-152>.

Foramitti, H., 1977. The unit of terrestrial photogrammetry working for the preservation of historical buildings in earthquake regions. *International Journal of Housing Science and its applications*, 2, 351-357.

Forlin, P., Gerrard C.M., Petley D.N., 2015. ArMedEa project: archaeology of medieval earthquakes in Europe (1000-1550 AD). First research activities. In: Blumetti AA, Cinti F, De Martini P, et al. (eds) 6th International Inqua Meeting on Paleoseismology, Active Tectonics and Archaeoseismology. 19-24 April 2015, Pescina, Fucino Basin, Italy, pp 166–169

Fujii, Y., Fodde, E., Watanabe, K., & Murakami, K. 2009. Digital photogrammetry for the documentation of structural damage in earthen archaeological sites: The case of Ajina Tepa, Tajikistan. *Engineering Geology*, 105(1-2), 124–133. <http://doi.org/10.1016/j.enggeo.2008.11.012>

Galeazzi, F., 2016. Towards the definition of best 3D practices in archaeology: Assessing 3D documentation techniques for intra-site data recording, *Journal of Cultural Heritage*, 17, 159-169. <http://doi.org/10.1016/j.culher.2015.07.005>

Gallo, A., Muzzupappa, M., & Bruno, F., 2014. 3D reconstruction of small sized objects from a sequence of multi-focused images. *Journal of Cultural Heritage*, 15(2), 173-182.

García Porras, A., 2001. La cerámica del poblado fortificado medieval de “El Castillejo” (Los Guájares, Granada), Granada

Green, S., Bevan, A., & Shapland, M., 2014. A comparative assessment of structure from motion methods for archaeological research. *Journal of Archaeological Science*, 46(1), 173–181. <http://doi.org/10.1016/j.jas.2014.02.030>

Grünthal, G. (ed.), 1998. European Macroseismic Scale EMS-98. Musée National d'Histoire naturelle, Luxembourg, 101

Guidoboni E., Comastri A., 2005. Catalogue of earthquakes and tsunamis in the Mediterranean area from the 11th century to the 15th century. Bologna

Hinzen, K.-G., Fleischer, C., Reamer, S. K., Schreiber, S., Schütte, S., & Yerli, B., 2011. Quantitative methods in archaeoseismology. *Quaternary International*, 242(1), 31–41. <http://doi.org/10.1016/j.quaint.2010.11.006>

Hinzen, K.-G., Cucci L., Tertulliani A., 2013. Rotation of objects during the 2009 L'Aquila earthquake analyzed with 3D laser scans and discrete-element models, *Seismological Research Letters*, 84(5): 745-751

Kázmér, M., 2015. Damage to ancient buildings from earthquakes. In: Beer, M., Patelli, E., Kougioumtzoglou, I., Au, I. S.-K. (eds): *Encyclopedia of Earthquake Engineering*, Springer, Berlin, pp. 500-506, 18 figs.

Kázmér, M., & Major, B., 2010. Distinguishing damages of two earthquakes – archeoseismology of a Crusader castle (Al-Marqab citadel, Syria). In: SINTUBIN, M. STEWART, I., NIEMI, T. & ALTUNEL, E. (eds): *Ancient Earthquakes*. Geological Society of America Special Paper, 471, 186–199.

Kázmér, M., Major B., 2015. Safita castle and rockfalls in the 'dead villages' of coastal Syria - an archaeoseismological study. – *Comptes Rendus Geoscience* 347, 181-190.

Malpica, A., Barceló, M., Cressier, P., Rosselló, G., Marín, N., 1985. Excavación de El Castillejo (Los Guájares, Granada), 1985, *Anuario Arqueológico de Andalucía 1985*, Sevilla, tomo II, 436-446

Malpica, A., Barceló, M., Cressier, P., Rosselló, G., Marín, N., 1986. Informe de la campaña de excavación sistemática del yacimiento medieval de El Castillejo (Los Guájares, Granada), 1985', *Anuario Arqueológico de Andalucía 1986*, Sevilla, tomo II, 487-492

Malpica, A., Cressier, P., 1989. Informe sobre la campaña de excavación sistemática de “El Castillejo” (Los Guájares, provincia de Granada). Año 1989', *Anuario Arqueológico de Andalucía 1986*, Sevilla, tomo II, 287-289

Marco, S., 2008. Recognition of earthquake-related damage in archaeo-logical sites: examples from the Dead Sea fault zone. *Tectonophysics* 453, 148–156.

Martínez, S., Ortiz, J., Gil, M. L., Rego, M. T., 2013. Recording Complex Structures Using Close Range Photogrammetry: The Cathedral of Santiago De Compostela. *The Photogrammetric Record*, 28(144), 375–395. <http://doi.org/10.1111/phor.12040>

Megaw, A. H. S., 1957. *Archaeology in Cyprus, 1957*, *Archaeological Reports* (The Society for the Promotion of Hellenic Studies), 4: 43-50

Megaw, A. H. S., 1972. ‘Supplementary excavations on a castle site at Paphos, Cyprus’, *Dumbarton Oaks Papers*, 26: 322-343.

Megaw, A. H. S. 1994. A castle in Cyprus attributable to the Hospital?, in Barber, M. (ed.) *The military orders: fighting for the faith and caring for the sick* (Aldershot: Ashgate).

Olson, B. R.; Placchetti, R. A.; Quartermaine, J., Killebrew, A. E., 2013. The Tel Akko Total Archaeology Project (Akko, Israel): Assessing the suitability of multi-scale 3D field recording in archaeology, *Journal of Field Archaeology*, 38 , 244-262

Peloso, D., 2005. Tecniche laser scanner per il rilievo dei beni culturali, *Archeologia e Calcolatori*, 16 , 199-224

Petre J. S., 2012. Crusader Castles of Cyprus: The Fortifications of Cyprus under the Lusignans, 1191–1489, Nicosia

Pollefeys, M., Koch, R., Vergauwen, M., & Van Gool, L., 2000. Automated reconstruction of 3D scenes from sequences of images. *ISPRS Journal Of Photogrammetry And Remote Sensing*, 55(4), 251-267. [http://dx.doi.org/10.1016/S0924-2716\(00\)00023-X](http://dx.doi.org/10.1016/S0924-2716(00)00023-X).

Pollefeys, M., Van Gool, L., Vergauwen, M., Cornelis, K., Verbiest, F., & Tops, J., 2001, , Image-based 3D acquisition of archaeological heritage and applications. In *Proceedings of the 2001 conference on Virtual reality, archeology, and cultural heritage*, 255-262. ACM. <http://dx.doi.org/10.1145/584993.585033>.

Rodríguez-Pascua MA, Pérez-López R, Giner-Robles JL, Silva PG, Garduño-Monroy VH, Reicherter K, 2011. A comprehensive classification of Earthquake Archaeological Effects (EAE) in archaeoseismology: Application to ancient remains of Roman and Mesoamerican cultures, *Quaternary International* 242, 20-30

Rodríguez-Pascua M, Silva P.G, Pérez-López R, Giner-Robles J.-L, Martín-González F, Perucha M.A, 2013. Preliminary intensity correlation between macroseismic scales (ESI07 and EMS98) and Earthquake Archaeological Effects (EAEs). In: Grützner C, Rudersdorf A, Pérez-López R, Reicherter K (Eds.), *Seismic Hazard, Critical facilities and Slow Active Faults. PATA Days. Proceedings of the 4th International INQUA Meeting on Paleoseismology, Active Tectonics and Archaeoseismology (PATA)*, 9–14 October 2013, Aachen, Germany, pp. 221–224.

Rosser, J., 1985. Excavations at Saranda Kolones, Paphos, Cyprus, 1981-1983, *Dumbarton Oaks Papers*, 39: 81-97.

Rosser, J., 1986. Crusader Castles of Cyprus, *Archaeology*, 39(4): 40-47.

Rosser, J., 2004. Archaeological and literary evidence for the destruction of “Saranda Kolones” in 1222, *Cyprus Research Centre Annual Review*, 30: 39-50.

Salonia, P., Leti Messina, T., Marcolongo, A., & Scolastico, S., 2009. Three focal photogrammetry application for multi-scale and multi-level Cultural Heritage survey, documentation and 3D reconstruction. In *Proceedings of The 22nd CIPA Symposium 2009*.

Sánchez-Aparicio, L. J., Villarino, A., García-Gago, J., & González-Aguilera, D., 2015. Non-Contact Photogrammetric Methodology To Evaluate the Structural Health of Historical Constructions. *ISPRS - International Archives of the Photogrammetry, Remote Sensing and Spatial Information Sciences*, XL-5/W4, 331–338. <http://doi.org/10.5194/isprsarchives-XL-5-W4-331-2015>

Sapirstein, P., 2016. Accurate Measurement with Photogrammetry at Large Sites, *Journal of Archaeological Science* 66 (February): 137–45. doi:<http://doi.org/10.1016/j.jas.2016.01.002>.

Stal, C., Van Liefferinge, K., De Reu, J., Docter, R., Dierkens, G., De Maeyer, P., Mortier, S., Nuttens, T., Pieters, T., van de Eijnde, F., van de Put, W. & De Wulf, A., 2014. Integrating geomatics in archaeological research at the site of Thorikos (Greece). *Journal of Archaeological Science*, 45, 112-125. doi:<http://dx.doi.org/10.1016/j.jas.2014.02.018>.

Schreiber, S., Hinzen, K.G., Fleischer, C., 2009. An Application of 3D Laser Scanning in Archaeology and Archaeoseismology: The Medieval Cesspit in the Archaeological Zone Cologne, Germany. 1st INQUA-IGCP-567. International Workshop on Earthquake Archaeology and Palaeoseismology, Baelo Claudia, Cádiz, Spain, 136-138.

Tapete, D., Casagli, N., Luzi, G., Fanti, R., Gigli, G., & Leva, D., 2013. Integrating radar and laser-based remote sensing techniques for monitoring structural deformation of archaeological monuments. *Journal of Archaeological Science*, 40(1), 176–189. <http://doi.org/10.1016/j.jas.2012.07.024>

Teza, G., Pesci, A., & Ninfo, A., 2016. Morphological Analysis for Architectural Applications: Comparison between Laser Scanning and Structure-from-Motion Photogrammetry. *Journal of Surveying Engineering*, 04016004. [http://doi.org/10.1061/\(ASCE\)SU.1943-5428.0000172](http://doi.org/10.1061/(ASCE)SU.1943-5428.0000172)

Yastikli, N., 2007. Documentation of cultural heritage using digital photogrammetry and laser scanning. *Journal of Cultural Heritage*, 8(4), 423–427. <http://doi.org/10.1016/j.culher.2007.06.003>

Acknowledgments

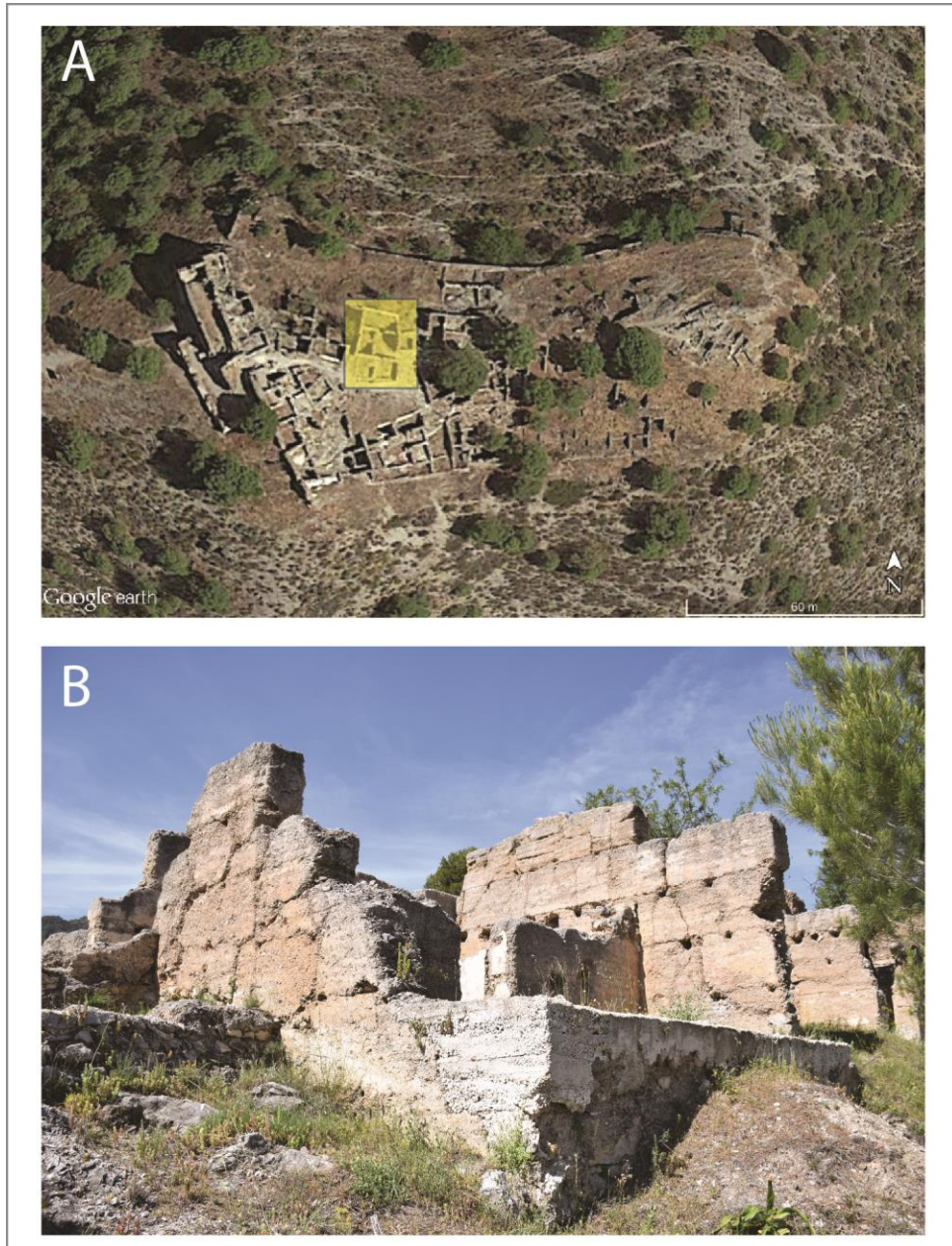
ArMedEa was developed in the Department of Archaeology and the Institute of Hazard, Risk and Resilience of Durham University and supported by a Marie Curie Intra European Fellowship (PIEF-GA-2013-626659) within the 7th European Community Framework Programme. Special thanks to Alberto Porras (University of Granada, Spain) and the Delegación de Cultura de la Junta de Andalucía for supporting the fieldwork undertaken in El Castillejo, and to the Department of Antiquities of Cyprus for supporting the research conducted in Saranda Kolones.

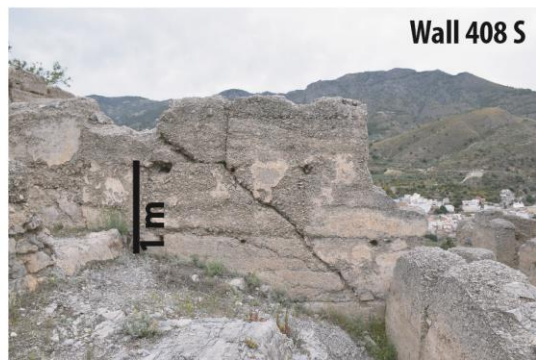
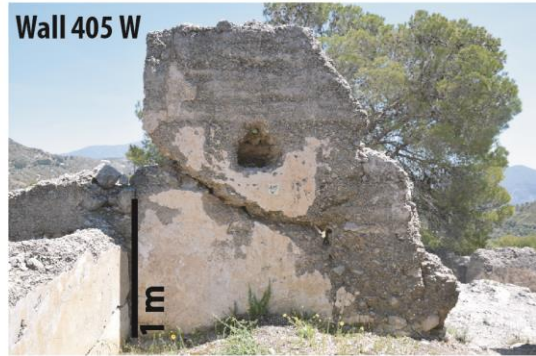
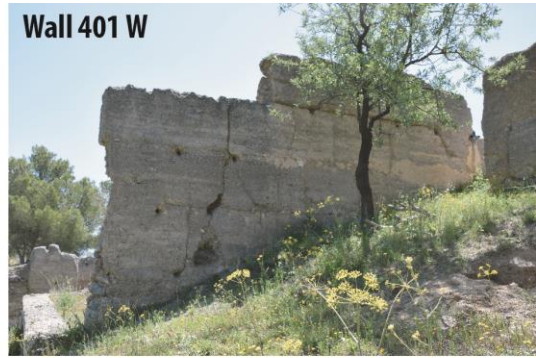
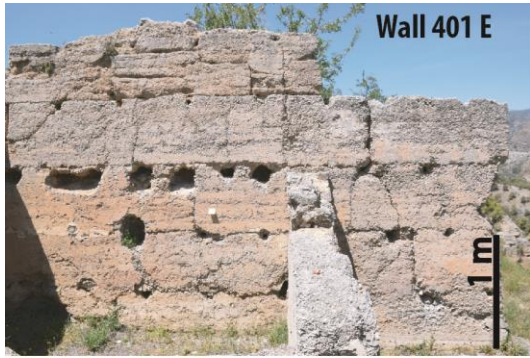
Paolo Forlin is particularly grateful to Dr Archibald Dunn (The Centre for Byzantine, Ottoman and Modern Greek Studies, The University of Birmingham) and Richard Anderson who kindly provided the instrumental survey of Saranda Kolones which was carried out as part of the ‘Saranta Kolones Excavations Project’. He also thanks Peter Brown and Elena Fiorin for taking part in the ArMedEa research conducted in Spain and Cyprus. Riccardo Valente would like to thank the Politecnico of Milan for supporting his staying at the Dept. of Archaeology of Durham University as PhD visiting student. He also thanks Luigi Barazzetti for his help with data processing

Table 1. Comparison between the measurements observed in the field and those extracted from the 3D meshes

Context	On-site measurements (mm)	Mesh Extracted measurements (mm)
El Castillo		
Displacement of <i>tapial</i> block in wall 401	Not accessible	45 (section B-B')
Crack depth inner face wall 405	~10	09 (section B-B')
Lower crack depth outer face wall 405	~20	35 (section B-B')
Saranda Kolones		
Pillar 2, lower displacement face W	23	25
Pillar 2, higher displacement face W	~30	33
Pillar 2, lower displacement face E	15	15
Pillar 2, higher displacement face E	~28	27



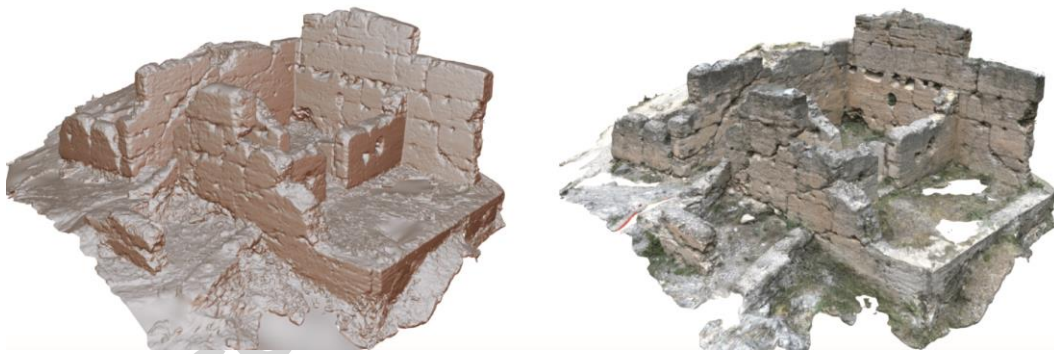
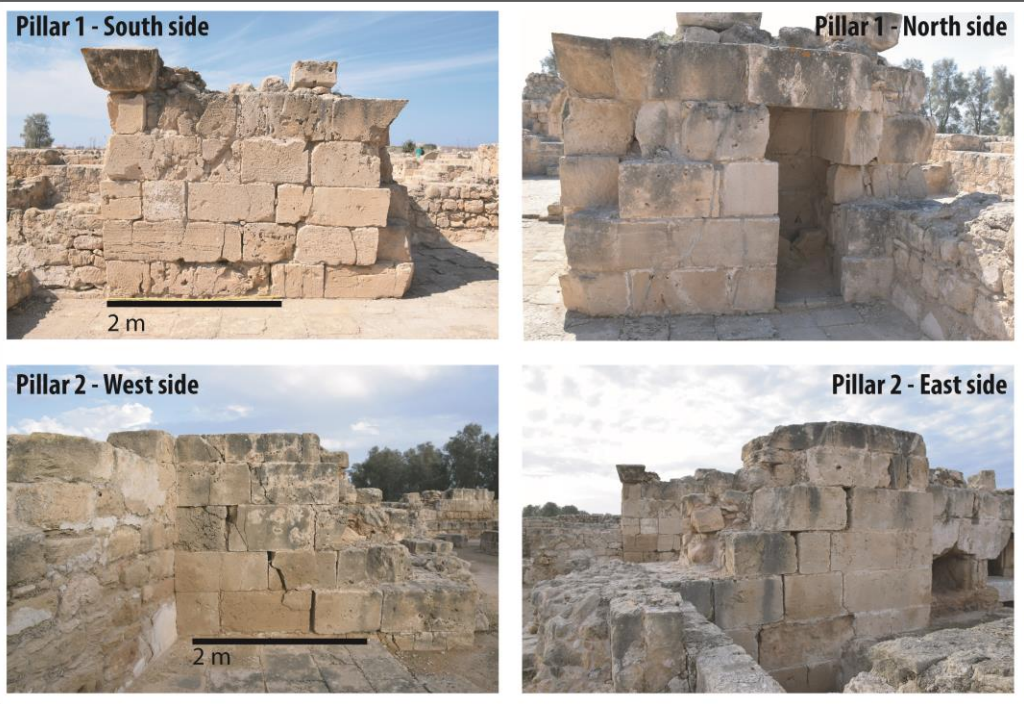


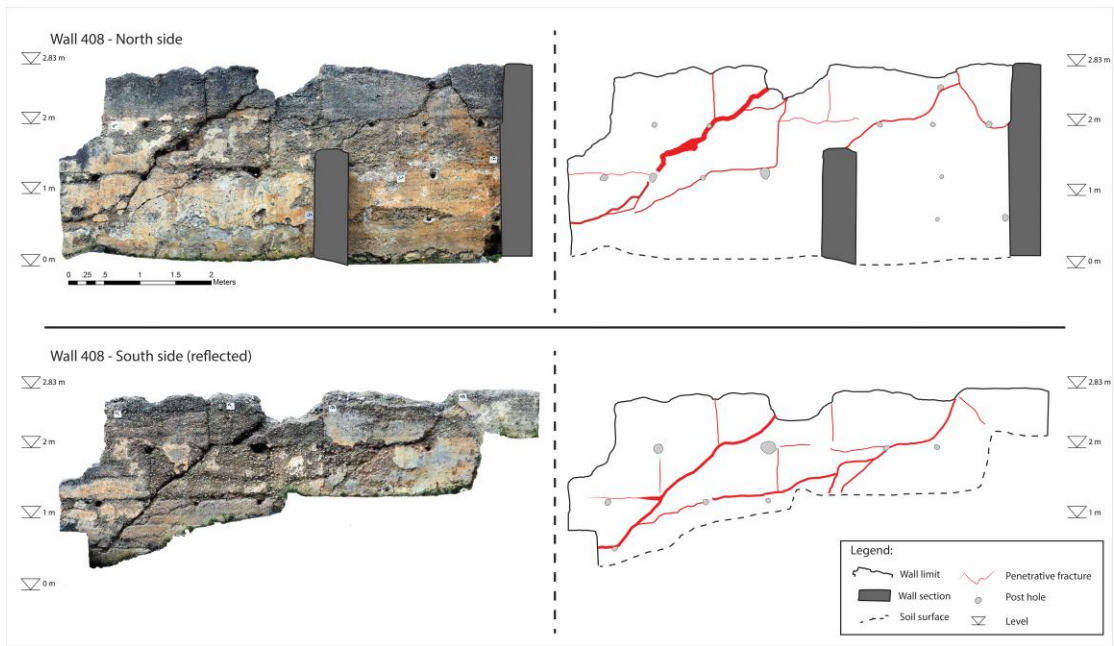


Accepted



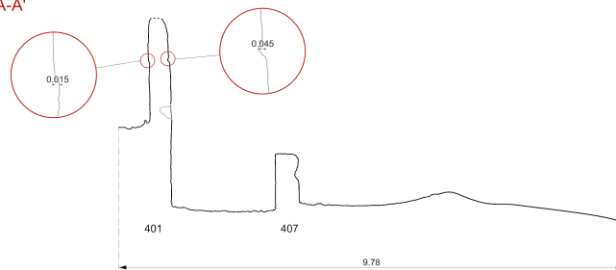
Accepted



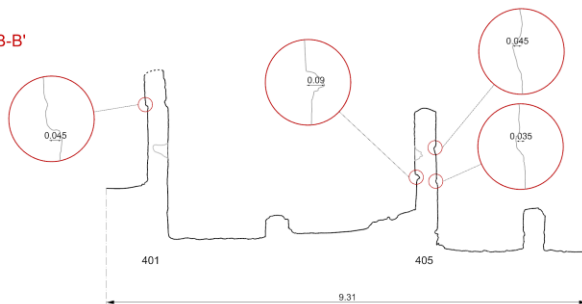


El Castillojo - Vertical Sections E/W

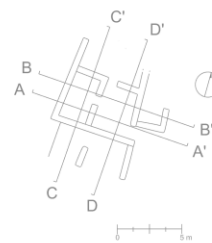
Section A-A'



Section B-B'

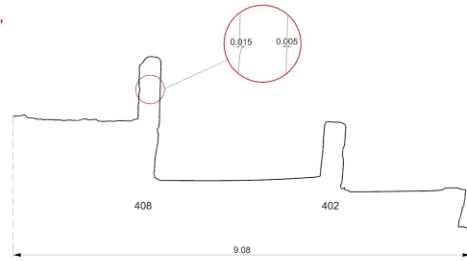


.....not surveyed

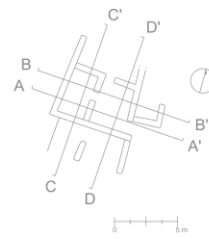
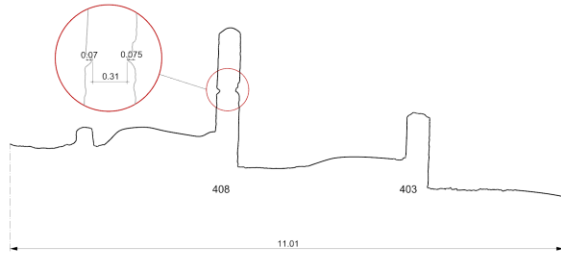


El Castillejo - Vertical Sections N/S

Section C-C'



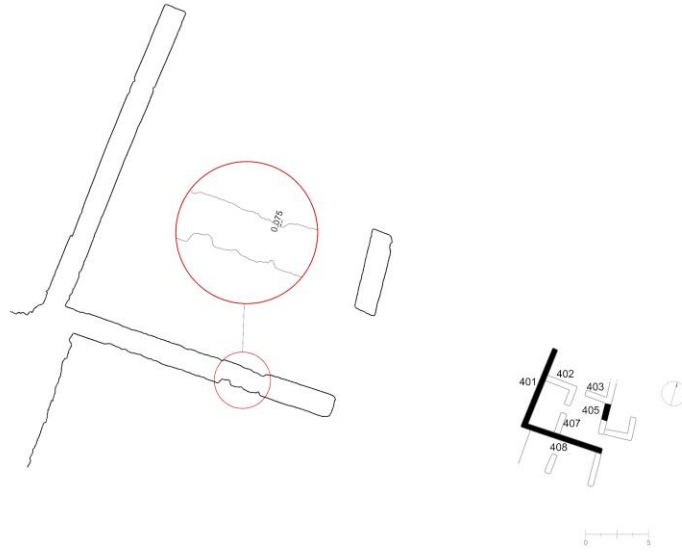
Section D-D'



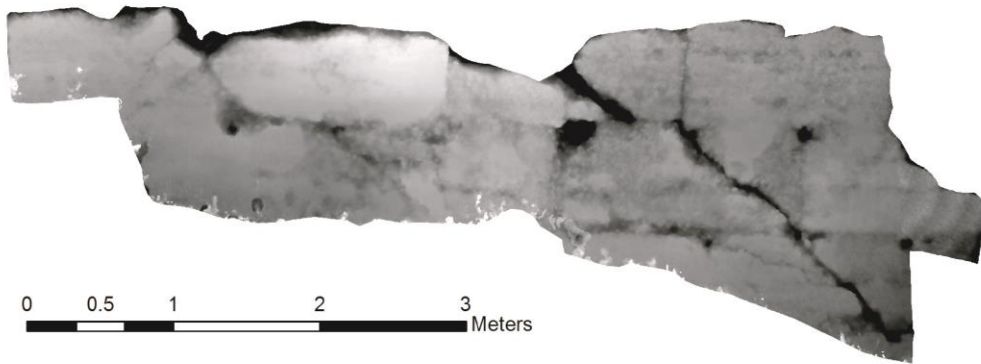
Accepted man.

El Castillejo Horizontal Section

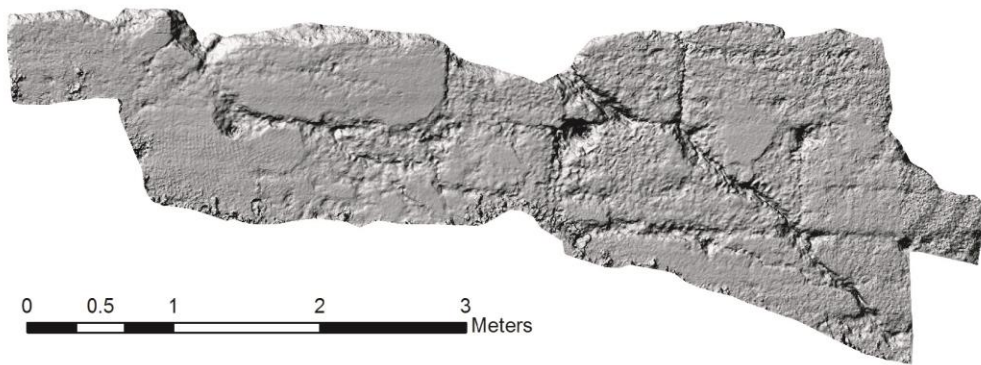
Section height: 2.12 m



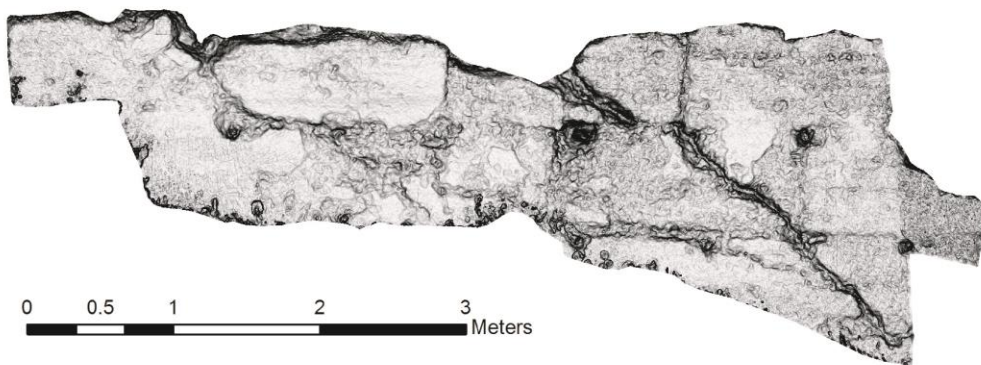
Accepted manuscript



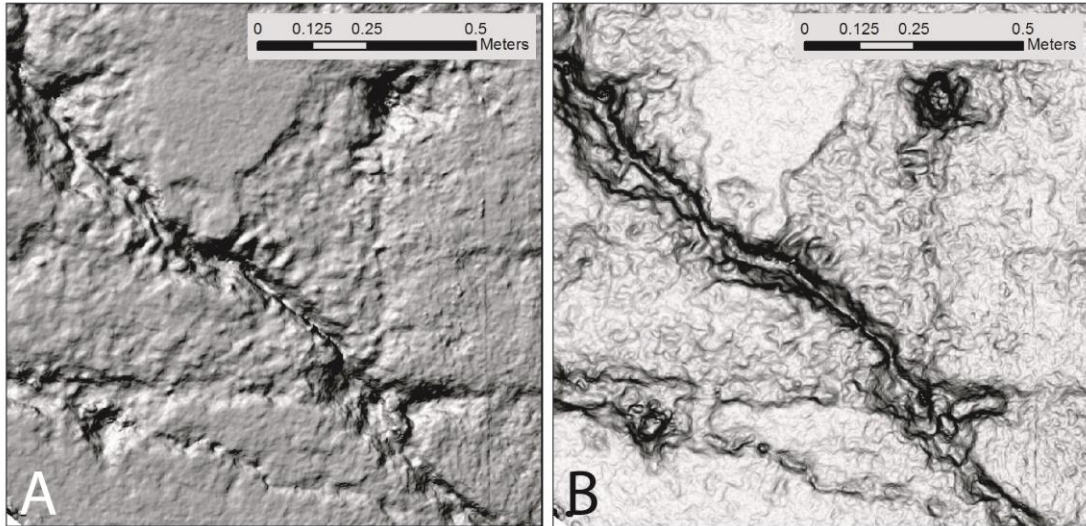
A



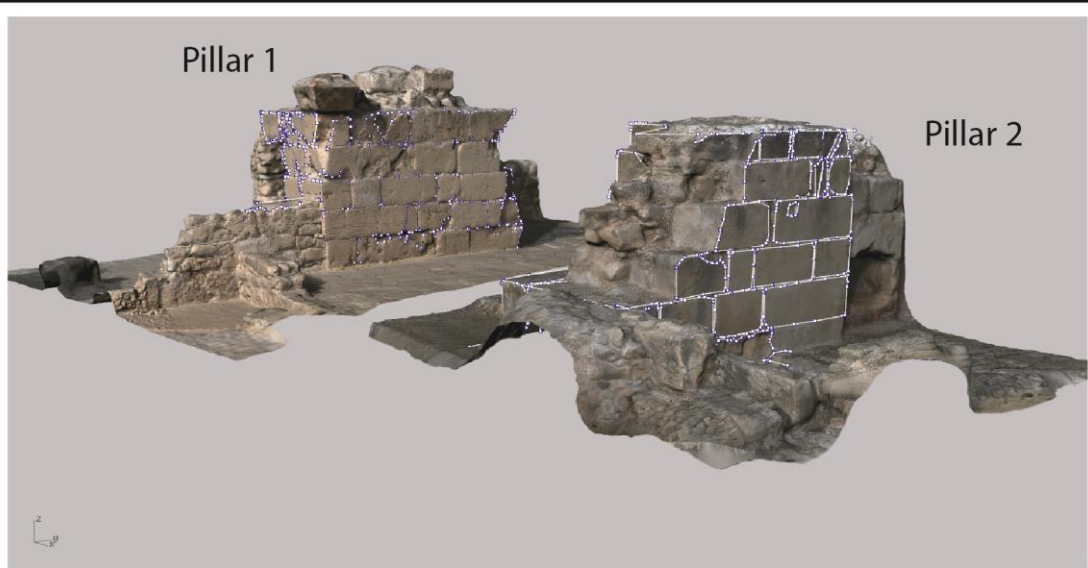
B



C



Accepted manuscript



Pillar 1 - face West



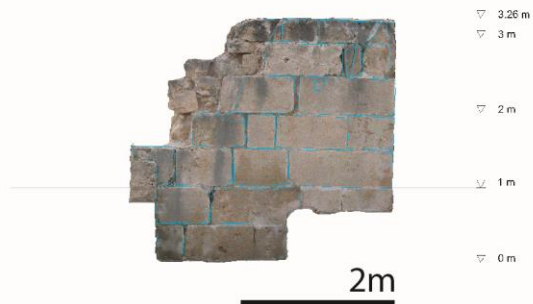
Pillar 1 - face East



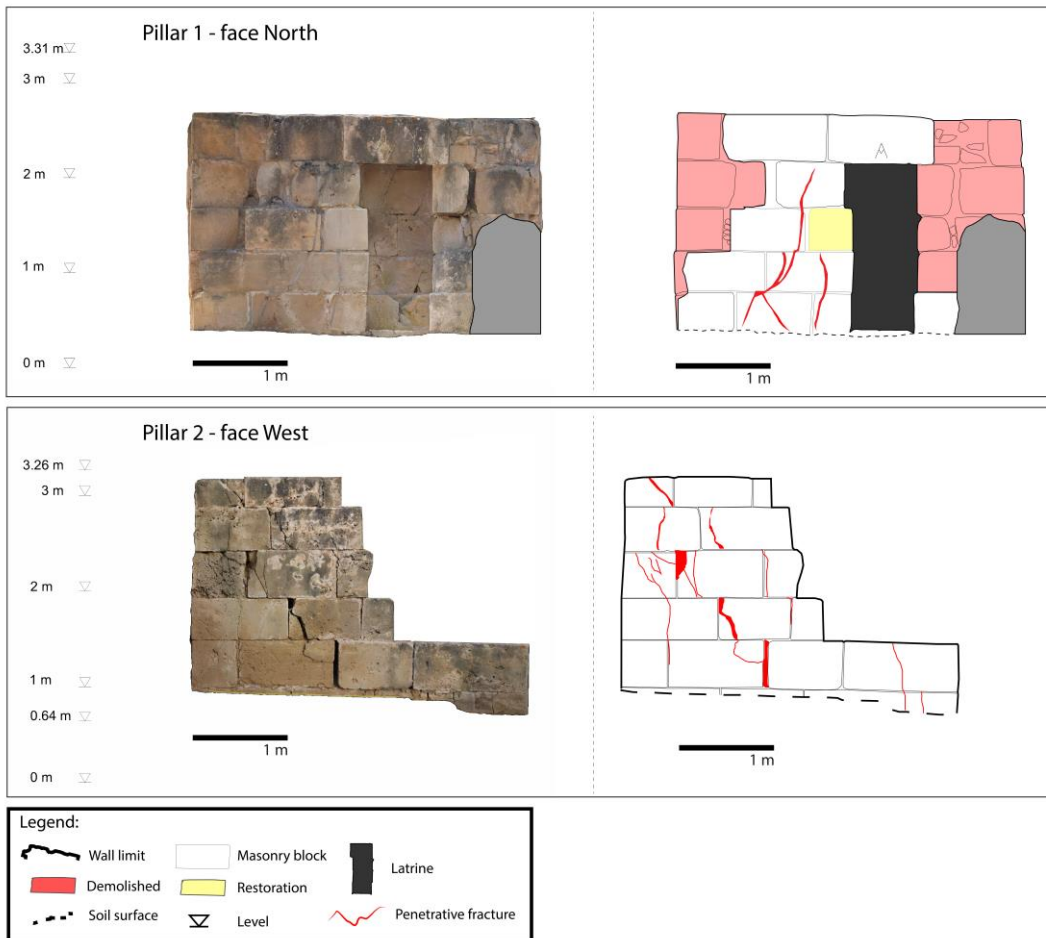
Pillar 2 - face West



Pillar 2 - face East



ACC





Saranda Kolones - Pilaster 2

